TSX-DATA FOR STUDIES OF SNOW ON ICE SHEETS AND SEA ICE – PRELIMINARY RESULTS

Wolfgang Dierking[1], Stefanie Linow[1], Christine Wesche[1], Wolfgang Rack[2], Mario Hoppmann[1], Sascha Willmes[3]

[1]*The Alfred Wegener Institute, Helmholtz Centre for Polar and Marine Research, Bussestr. 24, 27570 Bremerhaven, Germany, Wolfgang.Dierking@awi.de*
[2]*Gateway Antarctica, Center for Antarctic Studies and Research, University of Canterbury, Private Bag 4800, 8140 Christchurch, New Zealand, Wolfgang.Rack@canterbury.ac.nz*
[3]*Environmental Meteorology, University of Trier, Behringstraße 21, D-54286 Trier, Germany, willmes@uni-trier.de*

ABSTRACT

The balances between mass gain and loss of the ice sheets and of the polar sea ice have received increased attention because of their influence on changes of Earth's environment. In this context, investigations of snow accumulation on ice sheets and snow load on sea ice are important topics of recent research. This short note motivates the need for such investigations. First results addressing snow accumulation rates over Dronning Maud Land (Antarctica) and snow deposition on sea ice in Atka Bay (Dronning Maud Land) obtained from TSX images are presented.

1 Introduction

Considering the influence of climate change on the environmental conditions in the Polar Regions (and vice versa the effect of environmental changes in the Polar Regions on regional and global climate), the mass balances of ice sheets and sea ice need to be continuously monitored. The mass balances of the ice sheets, i. e. the difference between mass gain by snow accumulation and mass loss by melting processes and iceberg calving, affect, e. g., sea level variations and the freshwater flux into the ocean [1]. The mass balance of sea ice is reflected by variations of its extent, concentration (areal fraction of ice per unit area), drift, deformation, and thickness and has an impact on parameters related to climate, such as the albedo [2]. However, monitoring strategies are complex and require elaborate measurements including the use of different satellite sensors. Here, we discuss the role of the TSX mission in retrieving information about snow accumulation on ice sheets and snow load on sea ice. The former is of importance to estimate the gain of mass of the Antarctic and Greenland ice sheets as function of time and space, the latter plays an important role in the retrieval of sea ice thickness using laser or radar altimetry.

Over the ice sheets, the accumulation needs to be known over large areas. Ground measurements serve as calibration and validation points [3]. Satellite data from sensors with large spatial coverage and high temporal sampling rate (such as passive microwave radiometers) are used to interpolate between these points [4]. SAR data have been applied on regional and local scales [5]. The radar backscattering intensity depends on the snow/firn grain size and the thickness of the annual firn layers, besides firn density and temperature. (Firn is a transition stage between snow and glacial ice with densities of 400-830 kg/m^3.) Since large grain sizes and thin annual layers are characteristic for low accumulation, and small grains deposited in thicker layers are typical for high accumulation, radar can be used to indirectly measure accumulation rates. It is important to emphasize that the measured rates are averages down to depths determined by the penetration of the radar waves into the firn. For a detailed discussion of accumulation retrieval by means of SAR see Dierking et al. [5].

For measurements of sea ice thickness using Cryosat-2 (radar altimeter data), individual radar echoes reflected from the ground are separated into groups separating first-year and multi-year ice from open water and thin ice. The ice freeboard (i. e. the vertical distance between the ice surface and the water surface) is obtained by subtracting travel times over ice from travel times over water. The conversion of freeboard into ice thickness is carried out assuming hydrostatic equilibrium. Hereto, the average ice and water densities are needed as well as the snow mass per unit area on the ice [6].

2 Data

In the studies presented here we concentrate on Dronning Maud Land in Antarctica (western boundary 20°W, eastern boundary 44°38'E). The Atka Bay, which is a test site for studying snow on sea ice, is located at 70°35'S 7°51'W.

The objective of our investigations on accumulation rates on the ice sheets is to analyse whether multi-frequency and multi-polarization SAR data improve the retrieval of accumulation rates and provide additional insight into the interaction between radar waves and firn. Besides the ASAR images mentioned in [5], we used six RS-2 (Radarsat-2) images from January 2012 (quad-pol., five from ascending orbit, one descending, incidence angles 30.4°-32°, pixel size 25 m) and 18 TSX images acquired from February to April 2013 (stripmap HH- and VV-polarization, ten from ascending orbit, eight descending, incidence angles 27.5°-33.4°, pixel size 10 m). The images were acquired over the Kottas Traverse in Dronning Maud Land, for which in-situ measured accumulation data are available (see **Figure 1**).

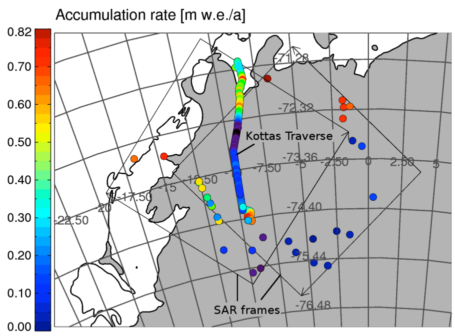

Figure 1 Accumulation rates along the Kottas Traverse and adjacent test sites. Also shown are the positions of two ASAR WSM-frames (ascending and descending orbit) used for the analysis.

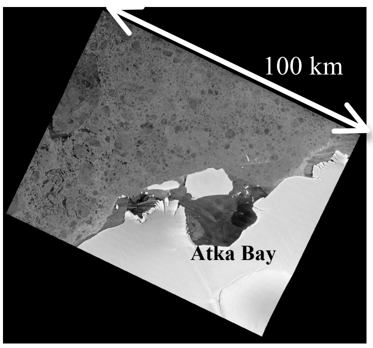

Figure 2 Fast sea ice in Atka Bay. The larger iceberg grounded at the northern border of the Bay is B15G. The elongated iceberg west of it is drifting.

For the study dealing with snow on sea ice we analysed four TSX-ScanSAR images (HH-polarization, incidence angles at image centre between 34.3° and 42.0°, pixel size 25 m) and eight scenes in stripmap-mode (4 HH+VV-pol., 2 HH+HV-pol., 2 HH single-polarization, incidence angles between 20.8° and 44.6°, pixel size 6 m). A TSX-ScanSAR scene from Atka Bay is shown in **Figure 2**.

3 Results

3.1 Kottas Traverse – Land Ice

The radar backscattering characteristics of firn depend on size, shape, orientation, volume fraction, and absorption loss of the scattering elements, and on the absorption loss of the background medium. In low-density firn closer to the surface of the ice sheets, scattering originates from snow grains, and the background medium is air. At larger depths, isolated air bubbles scatter the penetrating radar waves, whereas ice is the host medium. The volume

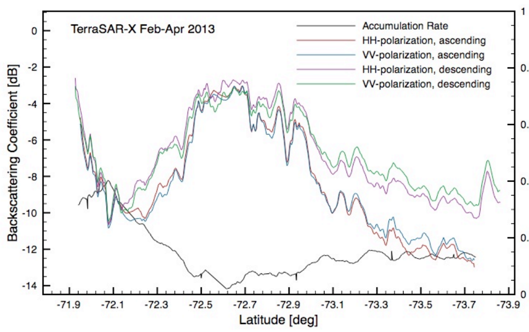

Figure 3 Radar backscattering coefficients measured at X-band (HH- and VV-polarization) along the Kottas Traverse from ascending (headings 321-326°) and descending orbit (214-219°) Also shown is the accumulation rate measured in-situ.

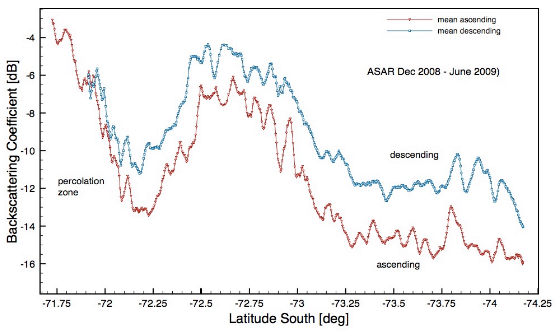

Figure 4 Radar backscattering coefficients measured at C-band (ASAR WSM, HH-polarization) over the Kottas Traverse from ascending (heading 344°) and descending (195°) orbit.

scattering contribution is usually calculated assuming that the scattering particles are of spherical shape [5]. Over the ice sheets, it is observed that the radar backscattering coefficient depends on look direction [7]. This azimuthal anisotropy is related to wave-like undulations of the ice surface on scales of decimetres to tens of metres (sastrugi). Since the surface scattering contribution of dry snow and firn is very low, it is assumed that also the surfaces from former years, which are buried under the most recent snow layers, contribute to the radar scattering.

In **Figure 3**, the backscattering coefficients obtained from TSX images along the Kottas-Traverse are depicted. They reveal a small difference between HH- and VV-polarization (0-0.5 dB) and a varying difference (0-3 dB) between ascending and descending orbit, with small values at low accumulation rates. For comparison, the results found at C-band HH-polarization (data source: ASAR WSM imagery) are shown in **Figure 4** . At low accumulation rates, the difference between ascending and descending orbit is between 0.5 and 3 dB, for higher rates, it varies between 3 and 5 dB. North of about 72.1°S along the Kottas traverse, the firn regime changes from dry snow to the percolation zone. In this regime, radar backscattering characteristics are more complex due to varying moisture content and the formation of ice lenses, pipes and channels in the firn volume.

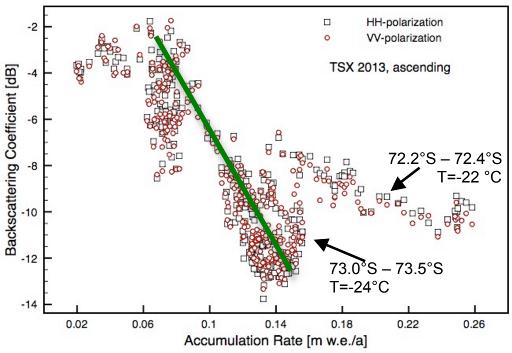

Figure 5 TSX-backscattering coefficients as a function of accumulation rate, measured along the Kottas-Traverse (ascending orbit).

One goal of our study is to find a relationship between measured radar parameters and the accumulation rate. In this context, we discuss the results presented in Figs. 5-7. In **Figure 5**, the X-band backscattering coefficients σ^0 at VV- and HH-polarization observed along the Kottas-Traverse are plotted as functions of the accumulation rate. For low accumulation rates (<0.05 m w.e./a) there is no recognizable sensitivity. At mid range (accumulation rates from 0.05 to 0.15 m w.e./a), σ^0reveals a strong gradient, indicated by the green line. However, in this case the data from the profile segment 72.2-72.4°S are excluded. They indicate a much weaker gradient. Since in dual-polarization stripmap mode of TSX, both channels are acquired coherently, we can also investigate the phase difference between the HH- and VV-polarized radar sinal. Over the Kottas Traverse, the phases are only weakly sensitive to the accumulation (for data from the ascending orbit even less than for descending orbit, see **Figure 6**). For comparison we show the corresponding result from RS-2 for which the phase sensitivity is much stronger.

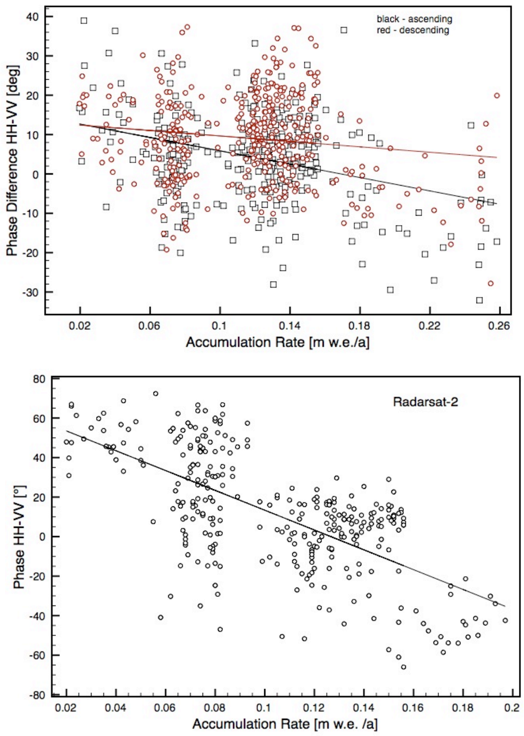

Figure 6 Phase difference between the HH- and the VV-polarized channel as a function of accumulation rate, measured along the Kottas Traverse. Top: from TSX-data (ascending and descending orbit). Bottom: from RS-2 (ascending orbit).

3.2 Atka Bay – Sea Ice

On the fast sea ice in Atka Bay, field measurements were carried out from November 2012 until January 2013. The data include snow thickness, depth profiles of snow temperature, density, and grain size, and ice properties at a number of test sites distributed over the frozen bay area. Snow thickness was highly variable (0-0.8 m). During a strong storm event, the snow was redistributed. Melt onset started in mid December.

The goal of this study is to assess whether properties of a snow layer on sea ice can be retrieved from radar data, and - if this is the case – under which conditions. In this initial phase of our study we focus on analysing radar signatures acquired for different surface and ice characteristics (sea ice type , surface roughness, snow properties). In **Figure 7**, cases are shown where the effect of snow, e. g. on the downwind side of an iceberg, can be recognized in TSX-images. It is interesting to note that the varying snow and ice properties are not only reflected in the radar intensity but also in the phase difference between the HH- and VV-polarized channel and the corresponding correlation (see **Figure 8**).

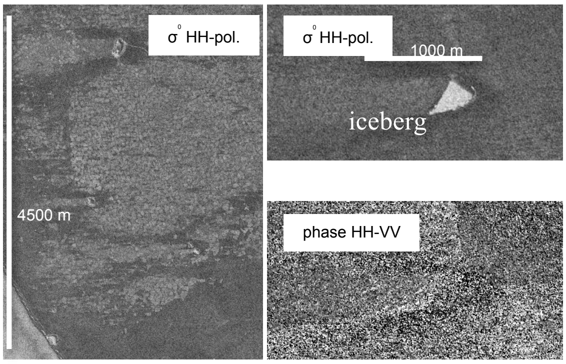

Figure 7 X-band backscattering coefficient at HH-polarization and phase difference HH-VV observed on fast sea ice in Atka Bay (TSX stripmap mode).

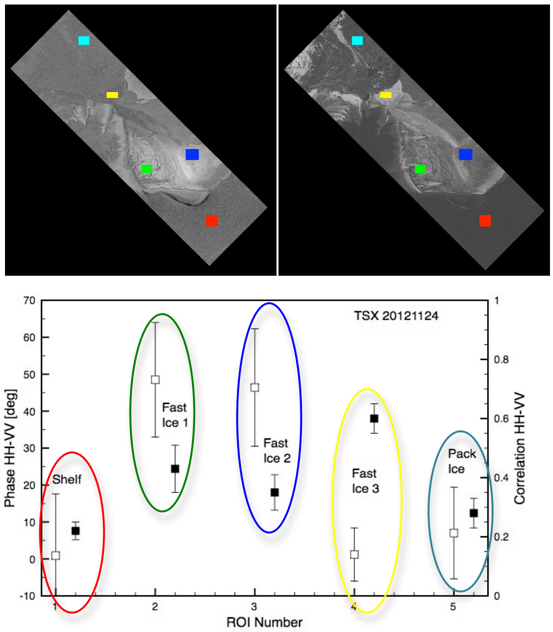

Figure 8 Phase difference and correlation between the HH- and VV-polarized TSX-signal over Atka Bay fast sea ice (test sites marked yellow, green and blue), pack ice (light blue) and the ice shelf (red). Black squares: correlation, white squares: phase.

4 Discussion

The TSX and RS-2 data acquired over the Kottas Traverse reveal a rather noisy pattern when plotted as a function of accumulation rate (Figs. 5 and 6), which poses a problem for developing a robust algorithm for retrieving average accumulation rates using SAR. Here further work is required for devising a method for pre-processing the SAR data. The sensitivities of the backscattering coefficient to accumulation rates at like-polarization are comparable at C- and X-band. At C-band the sensitivity at cross-polarization is larger than at like-polarization. The phase difference changes significantly as a function of accumulation rate at C-band but not at X-band. The reason for this sensitivity and the difference between C- and X-band needs to be analysed in detail. Also the differences of azimuthal anisotropy at C- and X-band will be studied further, taking into account the scene headings and radar penetration depths. For the Atka Bay, spatial and temporal variations of the TSX-backscattering signature have to be related to the snow and ice properties measured in the field. Our preliminary results indicate that phase difference and correlation between the HH- and VV-channel might give information about snow and ice conditions that is complementary to the radar intensity patterns.

Acknowledgement

Radar images were provided by projects TSX-OCE1592, TSX-MTH0123, and Radarsat-2 SOAR-EU 6766 which we gratefully acknowledge.

References

[1] Rignot, E., I. Velicogna, M. R. van den Broeke, A. Monaghan, and J. T. M. Lenaerts, *Acceleration of the contribution of the Greenland and Antarctic ice sheets to sea level rise*, Geophys. Res. Lett., 38, L05503, doi:10.1029/2011GL046583, 2011

[2] Serreze, M. C., M. M. Holland, and J. Stroeve, *Perspectives on the Arctic's shrinking sea ice cover*, Science, Vol. 315, 1533-1536, doi:10.1126/science.1139426, 2007

[3] Genthon, C., G. Krinner, and H. Castebrunet, *Antarctic precipitation and climate change predictions: horizontal resolution and margin vs plateau issues*, Annals of Glaciology Glaciology 50(50), 55-60, 2009

[4] Arthern, R. J., D. P. Winebrenner, and D. G. Vaughan, *Antarctic snow accumulation mapped using polarization of 4.3 cm wavelength microwave emission*, J. Geophys. Res., 111, D06107, doi:10.1029/2004JD005667., 2006

[5] Dierking, W., S. Linow, and W. Rack, *Towards a robust retrieval of snow accumulation over the Antarctic ice sheet using satellite radar*, J. Geophys. Res., 117, D09110, doi:10.1029/2011 JD017227, 2012

[6] Kwok, R., and C. F. Cunningham, *ICESAT over Arctic sea ice: Estimation of snow depth and ice thickness*, J. Geophys. Res., 116, C11018, doi:10.1029/2008JC005181, 2008

[7] Ashcraft, I. S., and D. G. Long, *Relating microwave backscatter azimuthal modulation to surface properties of the Greenland ice sheet*, J. Glaciol., 52(177), 257–266, doi:10.3189/172756506781828764, 2006